ACS OMEGA

http://pubs.acs.org/journal/acsodf

Article

Photocontrollable Crystallization at the Topological Defect of a Liquid Crystalline Droplet

Yota Sakai, Hinako Kusaki, and Kenji Katayama*

Cite This: *ACS Omega* 2021, 6, 35050−35056

Read Online

ACCESS | Metrics & More | Article Recommendations | Supporting Information

ABSTRACT: Photocontrollable crystallization at topological defects in a liquid crystal (LC) droplet was demonstrated. The molecules dissolved in a surfactant solution outside the LC droplet were moved into the droplet via light absorption. Nuclei emerged tens of seconds after light irradiation and moved toward the topological defect located at the droplet center, thus forming a branch-shaped crystal. This phenomenon was reproduced for multiple different molecules; photoinduced migration, nucleation, and crystal formation were discussed as a plausible mechanism.

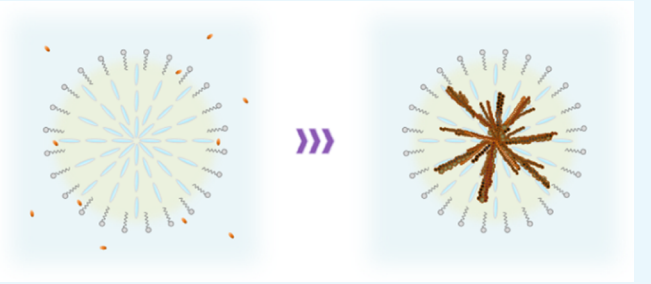

INTRODUCTION

Crystallization of chemicals is a fundamental process for materials from the perspective of basic science and practical applications. In a well-established theory by LaMer,[1] an oversaturated solution starts to provide nuclei for a crystal at the initial stages. Subsequently, the nuclei grow as long as the concentration of the chemical is oversaturated. For practical purposes, crystallization is necessary for the pharmaceutical industry, and it is also vital in basic science for the determination of the molecular structure of chemicals and proteins in the X-ray diffraction analysis.

However, many chemicals cannot be crystallized due to solubility, chemical interactions, impurities, limited amounts of materials, and so forth. Thus, much effort has been made in crystallization for preparing oversaturated concentrations via temperature, stirring speed, pH, and so forth.[2] For example, flow-based crystallization has been developed via control of an antisolvent and an introduction of plug flow.[3−5] As a unique technique, a porous metal−organic framework was used to absorb guest molecules and orient them in a crystalline form, that is, the "crystalline sponge method".[6,7] Laser-induced nucleation and crystallization have also been demonstrated and studied for some proteins.[8,9]

The liquid crystal (LC) is a phase between the solid and liquid—it has a periodic structure in a specific direction like a crystal and has fluidity in another direction like a liquid. This phase can be frequently found in living matter.[10] It plays a role in self-organization and structure formation for mechanical strength, color modification, and morphology. We can also find it in use for display purposes in our daily life.

Topological defects in LCs are actively studied because they can potentially control the structure and motion of LCs. Topological defects are an orientationally disordered point of LC molecules where the molecular orientation cannot be defined. Intentionally formed topological defects by the photoalignment layer can control the alignment of LCs and can be utilized for various thin optics.[11−13] A droplet made of LC has topological defects inside and on the surface,[14] and the droplets and spheres have been intensively studied as an "active matter", that is, the object could move around like a living object. The motion of LC spheres was controlled by the topological defects, which also caused molecular self-assembly.[15] Topological defects were further investigated in biology because biological cells aligned like LC molecules and had topological defects. Furthermore, they could control the collective motion and biological activity depending on the types of defects.[16,17]

The defects in LCs can sometimes help align and assemble colloids and molecules. Amphiphilic molecules were self-assembled to form nanostructures at the line defect (disclination).[15] LC ordering can align gold nanorods to the alignment direction in a lyotropic LC,[18] and gold nanoparticles were concentrated at the dislocation of the smectic LC.[19,20] The force induced by the disclination line and colloids is regarded as a new type of force.[21] The defect-induced assembly was observed for dense colloid particles in LCs,[22] and the disclination was intentionally controlled to make knots and links to form self-assembly of colloids.[23]

In this study, we accidentally found a unique crystallization phenomenon while studying a new category of active matters consisting of LCs.[24−26] During this study, we found that

Received: October 17, 2021
Accepted: November 30, 2021
Published: December 9, 2021

https://doi.org/10.1021/acsomega.1c05816
ACS Omega 2021, 6, 35050−35056

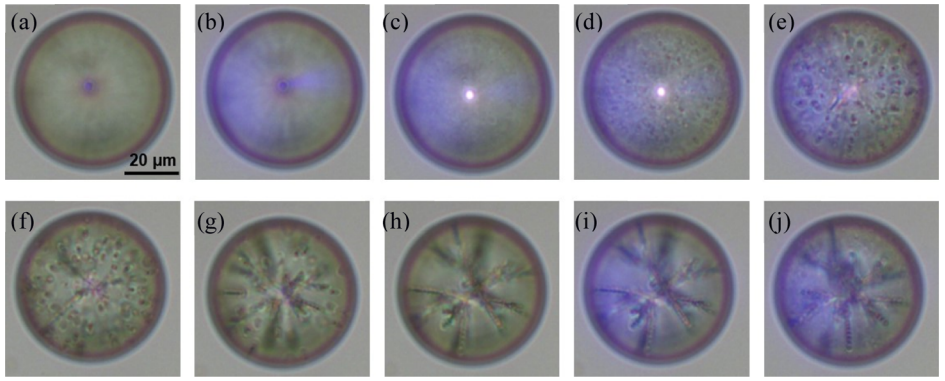

Figure 1. Snapshots of a 5CB droplet in an SDS solution with *p*-nitrophenol (0.01 wt %) under the on−off operation of the UV light: (a) before irradiation; (b−e) 0, 30, 60, and 90 s after the UV light was turned on; (f−h) 0, 60, and 120 s after the UV light was turned off; and (i,j) 0 and 30 s after the UV light was turned on again, respectively.

crystallization of a solute was triggered by light at the topological defect in a pure LC droplet even though the solute was dissolved outside the LC droplet. A crystal was formed inside the LC droplet when using light irradiation at a wavelength that matches the absorption of the solute. It grew at the center of the droplet (topological defect) with a branched shape. This is the first demonstration of the topological defect-induced crystallization under geometrical frustration.[27] In this paper, we demonstrate the formation of several crystals made of different solutes and describe possible mechanisms underlying this phenomenon.

RESULTS AND DISCUSSION

Figure 1 shows an image sequence of a 5CB droplet surrounded by a sodium dodecyl sulfate (SDS) solution with *p*-nitrophenol (0.01 wt %) during the on−off operation of a UV light. The droplet had a topological defect at the center, which is determined by the 5CB molecular alignment dominated by the boundary condition of the 5CB and the SDS solution (homeotropic alignment).[28] Unexpectedly, we observed that small objects (∼2 μm) started to nucleate inside and around the boundary of the droplet in about 30 s (Figure 1c) and became larger (Figure 1d−f). Simultaneously, these objects were attracted to the center of the droplet, i.e., to the topological defect. The objects were gradually connected to grow and shaped a branched structure. When the light was turned off, the small nucleated objects slowly stopped to generate. These processes were repeated when the UV light was turned on again, and nucleated objects were connected to the original branches to make additional branches (Movie S1 in the Supporting Information).

This nucleation, growth, and the subsequent structure formation inside the LC droplet was observed under the crossed-Nicols condition (Movie S2 in the Supporting Information). Figure 2a,b shows the snapshots of the 5CB droplets before and after the nucleation and growth by irradiation of the UV light, respectively. Under the crossed-Nicols observation, the LC droplet showed a crossed texture (Figure 2a) known as a radial pattern, which indicates that the long axis of the molecules was oriented in the radial direction determined by the anchoring condition via the outside SDS molecules.[14,29] The generated branched structure showed black lines along the branch direction; each branch was sandwiched by whitish covers as shown in Figure 2b. This result indicated that this object has polarization characteristics,

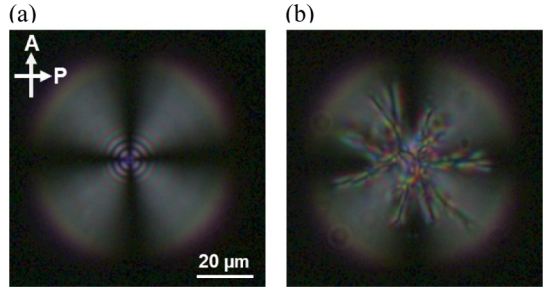

Figure 2. Snapshots of the 5CB droplet in an SDS solution with *p*-nitrophenol (0.01%) observed via a polarization microscope under the crossed-Nicols condition: (a) before irradiation and (b) after UV irradiation for 60 s. The white arrows in (a) indicate the direction of the analyzer and the polarizer.

suggesting ordered alignment of molecules because the same color indicates the same orientation of the unit structure. The molecules are aligned either in the polarizer or analyzer direction in the black region; they are in-between in the white regions. The specific color was observed in the whitish regions, indicating that a periodic structure induces color interference. This result strongly suggests that the structured object was made of a crystalline state in which molecules were aligned in particular directions.

These phenomena were observed for alizarin yellow GG and chrome yellow (Figure 3a,b) (Movie S3a,b in the Supporting Information). We found the nucleation, growth, and formation of the branched structure again for these molecules, and the only difference was the formation speed of the branched structure. The requirement was that the molecules need to have absorption at the wavelength of the illumination light (365 nm). We could successfully observe similar phenomena for various solutes, *o*-nitrophenol, *m*-nitrophenol, allura red AC, naphthol yellow S, martius yellow, and orange G with absorption at 365 nm (Figure S1 in the Supporting Information). However, we did not observe the formation of objects for new coccine (λ_{max} ∼ 500 nm) or sunset yellow (λ_{max} ∼ 480 nm), which do not have a major absorption band at the illumination source.

We could not take out the crystal from the droplet because the droplet collapsed during the evaporation of solvents. Raman microscopy (magnification: ×40) was used for the characterization of the photogenerated crystals inside the LC droplet. The crystal inside the 5CB droplet was measured

https://doi.org/10.1021/acsomega.1c05816
ACS Omega 2021, 6, 35050−35056

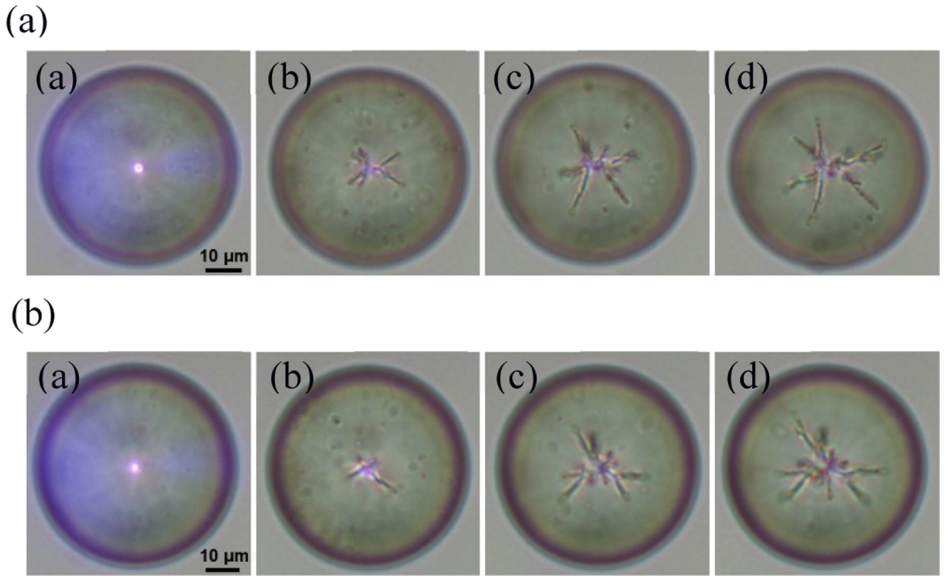

Figure 3. Snapshots of the 5CB droplet in an SDS solution including (a) alizarin yellow GG and (b) chrome yellow under the on−off operation of the UV light. (a) just after the UV irradiation and (b−d) 120, 240, and 480 s after the UV light was turned on.

under the same experimental conditions as the formation of this object. Pure 5CB in the LC phase, pure *p*-nitrophenol (powder), and an SDS solution with *p*-nitrophenol were measured for comparison (Figure. S2 in the Supporting Information). The lateral resolution of the microscope was about 1 μm, but no specific depth resolution is guaranteed; the spectrum includes information on the crystal and the droplet medium. The Raman peaks at 420.9, 646.6, 789.2, 820.1, 838.7, and 1033.5 cm^{-1} correspond to 5CB and 874.4 and 1129.0 cm^{-1} were for *p*-nitrophenol. Obviously, the mixed spectra of 5CB and *p*-nitrophenol were observed for the droplet including the photogenerated crystal, which was assigned as *p*-nitrophenol. The Raman spectrum was not obtained for *p*-nitrophenol dissolved in an SDS solution under the same experimental conditions. We could not exclude the possibility of the formation of a cocrystal of 5CB and *p*-nitrophenol,[30] but it is not likely considering that various molecules with different structures were subject to form the object, as shown in Figure S1 in the Supporting Information.

The chemical source formed inside the droplet was initially dissolved in the outer solution. The temporal change of the UV/Vis absorption spectrum of the outer solution was measured during UV irradiation to investigate the amount change of the chemical source in the outer solution. A single 5CB droplet with a volume of 20 μL was prepared in a 0.3 wt % SDS solution with 0.001 wt % *p*-nitrophenol (10 mL) in a vial. The outer SDS solution was sampled (0.5 mL every 30 s) during the UV irradiation, and the absorbance of each sample was measured by a UV/Vis spectrometer.

The spectra for the different sampling times during the UV light irradiation are shown in Figure 4. The absorption peak at 316 nm for *p*-nitrophenol (Figure S7) gradually decreased during UV irradiation. This result indicates that the amount of *p*-nitrophenol in the outer SDS solution decreased during light irradiation. This result suggests that the molecules migrated from the outer solution into the LC droplet, which was the source of the nucleated crystal. The same experiments were performed without the light illumination (Figure S3a) and without a 5CB droplet (Figure S3b). The concentration change of *p*-nitrophenol in the solution was negligible.

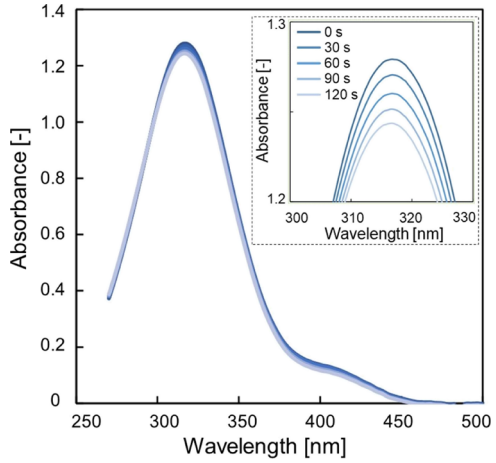

Figure 4. Temporal change of the UV/Vis absorption spectra of the outside SDS solution with *p*-nitrophenol (0.001%) including a 5CB droplet during the UV light irradiation. The outside solution was sampled every 30 s during UV light irradiation.

The interfacial tension was monitored during the light irradiation to obtain further evidence for the transfer of the solute molecules at the interface between the LC droplet and the SDS solution. The interfacial tension change during the on−off operation of the UV light was monitored via the pendant drop measurements of the LC droplet in an SDS solution with *p*-nitrophenol (Figure 5). The UV light was irradiated for 20 s twice. The interfacial tension gradually increased during the UV irradiation and decreased after being turned off. Although the absolute value of the interfacial tension fluctuated due to the sensitivity of the measurement, the tendency of the increase by the light irradiation was always reproduced. This result indicates the desorption of molecules from the LC/water interface during UV irradiation. This desorption process is interpreted by the desorption of the solute molecules initially adsorbed at the LC/water interface into the LC phase. The interfacial tension change due to the temperature rise (<0.8 °C) can be neglected.

https://doi.org/10.1021/acsomega.1c05816
ACS Omega 2021, 6, 35050−35056

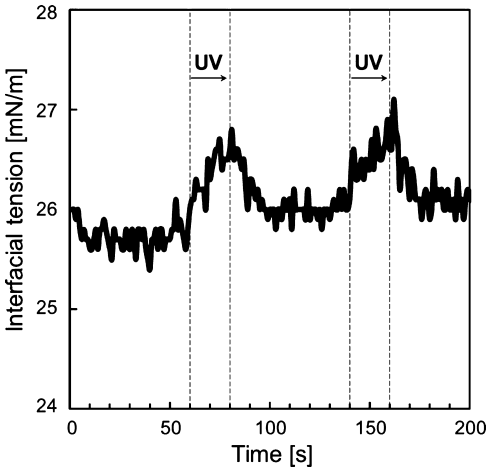

Figure 5. Change of the interfacial tension during the on−off operation of the UV light for a 5CB droplet in an SDS solution with *p*-nitrophenol (0.01 wt %). The UV light was irradiated twice for 20 s at 60 and 140 s during the measurement.

The interfacial tension monitoring suggested that solute molecule desorption was promoted from the interface by light—this, in turn, indicates that the solute molecules were initially adsorbed at the LC/water interface. The contact angle of an LC droplet on the solute concentration in the outer solution was studied to verify this hypothesis. A 20 μL drop of 5CB was placed onto a hydrophobically treated Petri-dish. The contact angles of the 5CB droplets surrounded by 0.3 wt % SDS solutions (0, 0.1, and 0.5 wt % *p*-nitrophenol) were measured. Pictures of each droplet are shown in Figure S4 in the Supporting Information. The contact angle decreased as the solute concentration in the outer solution increased, indicating a decrease in the interfacial tension. This result indicates that solute molecules adsorb at the interface in a static state, supporting our assumption.

The mechanism of the solute solubilization into the LC droplet has not been clarified. Organic molecules dissolved in an aqueous surfactant solution are usually solubilized into the organic phase as a reverse micelle. We hypothesized that SDS molecules form reverse micelles of the solute molecules to solubilize the material into the LC phase. The effect of the reverse micellar solubilization was studied by changing the type of surfactant. Instead of SDS, we used polyvinyl alcohol (PVA) as a protecting agent for the LC droplet. PVA could maintain the stability of the LC droplet interface via a random coil formation, but this does not make a reverse micelle for the solute molecules.[28] A 5CB droplet was prepared in a PVA solution (1 wt %) with 0.01 wt % *p*-nitrophenol, and the UV light was similarly illuminated. The result is shown in Figure 6 (Movie S4 in the Supporting Information). The nucleation of small objects started inside the LC droplet about 30 s after the UV light irradiation, which is similar to the phenomena for the SDS solution. This result indicates that reverse micellar solubilization was not a necessary process for transferring the solute molecules into the LC phase. We assumed that solutes were taken up into the LC phase on their own from this result.

The above experiment offered another important piece of information on this crystallization process. Movie S4 and Figure 6 show that the small nuclei did not approach the droplet center even though the solute nucleation was also induced in a PVA solution. The nucleated and grown small objects kept fluctuating inside the LC droplet. PVA imposes a planar orientation of the LC molecules (parallel) at the LC/solution interface, and the LC alignment in the droplet adopts a bipolar configuration where two topological defects are formed at each pole and do not have one in the center.[14,28] This result strongly suggests that the topological defect at the center or the radial alignment of the LC droplet has a crucial role in the buildup of the crystalline phase.

This result was supported by the experiment when we used a droplet in the isotropic phase by increasing the temperature >35 °C. The behavior of the droplet under the light illumination is shown in Movie S5 in the Supporting Information. The nucleation of small objects started inside and the LC droplet under the UV light irradiation, but they did not form a branch-shaped object, similar to the result in Figure 6. This result supports the assumption that the requirement for the branched structure is the existence of the topological defect at the center, but the nucleation itself was determined by the properties of LC.

The effect of the LC phase on the nuclei formation was investigated from the observation of the oil droplet behavior (toluene droplet) under the same experimental conditions (Movie S6 in the Supporting Information). No reactions proceeded during the light irradiation. This result shows that the LC phase was necessary to take up the solute molecules into the LC phase or for the nucleation itself. Furthermore, we investigated the temperature influence for the crystallization because the photoabsorbed molecules release heat via photothermal relaxation and/or photoisomerization in the case of azo dyes. The behavior of the 5CB droplet in an SDS solution with *p*-nitrophenol was observed under a temperature variation in a temperature-controlled vessel, where the temperature was controlled at the thermocouple attached to the sample cell. The temperature was initially set at room temperature (25 °C) and was increased by 5 °C, which is sufficiently higher than the temperature rise estimated from the molar absorptivity at 365 nm of *p*-nitrophenol and the sample volume (~0.8 °C). Unexpected focusing of light due to the droplet could possibly increase the temperature of droplets, but we could ignore this because no phase transition was

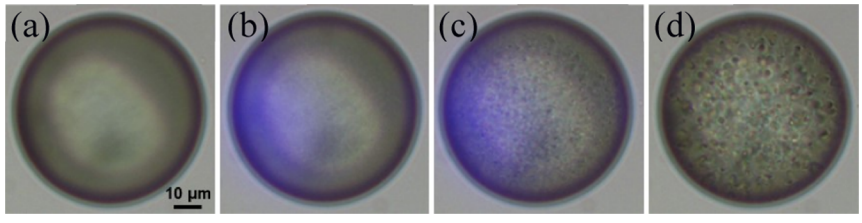

Figure 6. Snapshots of the 5CB droplet in a PVA solution with *p*-nitrophenol (0.01 wt %) under the UV on−off operation: (a) before UV irradiation; (b,c) 30 and 90 s after the UV light turned on, respectively; and (d) 60 s after the UV light turned off.

https://doi.org/10.1021/acsomega.1c05816
ACS Omega 2021, 6, 35050−35056

observed. The sample was then lowered to room temperature again (Movie S7 in the Supporting Information). No reaction was observed, and only the focus point was defocused under the temperature variation. This result shows that photoexcitation has a role in the crystallization process (causing uptake into the LC phase).

From these observations and considerations, we suggest the following crystallization mechanism: Some of the solute molecules were initially adsorbed at the LC/water interface as confirmed by the interfacial tension dependence on the solute concentration. Based on the dynamic interfacial tension measurement, the desorption of these solute molecules into the LC phase was promoted during the UV light irradiation. The molecules could be provided from the outside solution. The process would gradually increase the concentration of the solute molecules inside the LC droplet. We could not determine why the injection of the solute molecule into the LC phase was triggered by light irradiation, but one possibility is that the photoinduced dipole in the excited state prefers the LC environment. This uptake could be a similar process to the gold nanorods with a large dipole moment that were taken and aligned by LCs to show a long-range ordering.[18]

Quantum chemical calculation was performed to clarify the change of the molecular properties of *p*-nitrophenol. The dipoles in the ground state and the first excited state were calculated by TDDFT calculation using the 6-31G(d) basis set, and the results are shown in Figure S5. The dipole was changed from 5.73 debye in the ground state to 5.12 debye in the excited state. One of the possibilities is that the smaller dipole prefers the LC environment compared with the polar solvent, an aqueous surfactant solution. The same tendency of the dipole reduction in the excited state was confirmed for *o*-nitrophenol and *m*-nitrophenol.

The molecules start to form nuclei at random positions after overcoming the saturation concentration of the solute molecules. From Movie S4, no clear position dependence for the nuclei formation was confirmed, and it is supposed that the nucleation was caused under the supersaturated condition. The nuclei then gathered to the topological defect at the center and grew with a branched shape. The accumulation of objects to the LC defects (dislocation) was previously observed[15,19,20] where a preferable environment for assembly of objects is provided by reducing the high free energy core of the LC defects.[15] In our case, the nuclei were collected at the point defect at the center. The object can retain the crystalline phase confirmed by the crossed-Nicols observation, and this suggests that the LC provided a preferable environment for molecular orientations suitable for crystal growth. Pure LC molecules in the LC phase could work as a metastable state inducing frustration for the crystal formation. The LC phase could potentially ease the nucleation of molecules via an ordering environment for extraneous molecules[27] similar to crystal sponge.[6]

CONCLUSIONS

We report a photocontrollable unique crystallization process at the topological defect of an LC droplet in a surfactant solution including solute molecules. The solute molecules were initially adsorbed at the interface of the droplet/surfactant solution and were desorbed into the LC droplet during light irradiation. The solute molecules overcame the saturated concentration inside the LC droplet and started to form crystal nuclei at random positions. These crystals gathered to the topological defect and grew with a branched shape in a crystalline form. This process was demonstrated for several different solute molecules with light absorption matching the irradiated light source. This is a brand new crystallization technique that is controllable by light. This process emphasizes the interesting role of topological defects. This is a simple and easy method for crystallization and can crystallize various molecules for pharmaceutical purposes and structural analyses.

METHODS

LC droplets were prepared using a microfluidic device. A schematic drawing of the device is shown in Figure S6 in the Supporting Information, and a detailed method is described. The typical size of the droplets was 50 μm in diameter.

4-cyano-4′-pentylbiphenyl (5CB, nematic phase: 22.5−35 °C) and 4-cyano-4′-heptylbiphenyl (7CB, nematic phase: 30−43 °C) were used as an inner fluid and an LC material (Figure 7a), and we only showed the result of 5CB because the results were similar for them. A SDS (0.3 wt %, 25 °C) solution was used as an outer fluid. The solution included water-soluble molecules whose absorption wavelengths have an overlap at 365 nm corresponding to the UV-LED wavelength. The solute molecules were *p*-nitrophenol, alizarin yellow GG, and chrome yellow; their molecular structures are shown in Figure 7b−d, respectively. Their absorption spectra are shown in Figure S7 in the Supporting Information. A schematic drawing of the observation setup is shown in Figure S8 in the Supporting Information. The droplet behavior was observed by an inverted microscope with a UV light illumination from the top side. Because the droplet diameter was much larger than the depth of focus, the optical images were blurred at some parts. We adjusted the focal position and the illumination light intensity

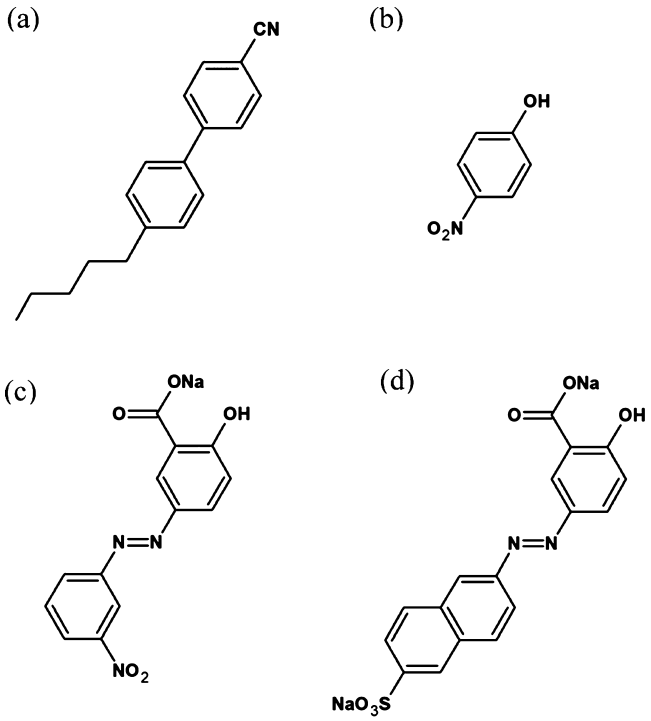

Figure 7. Molecular structures of the LC and the solute molecules. The solute molecules were dissolved in a surfactant solution: (a) 4-cyano-4′-pentylbiphenyl (5CB), (b) *p*-nitrophenol, (c) alizarin yellow GG, and (d) chrome yellow.

https://doi.org/10.1021/acsomega.1c05816
ACS Omega 2021, 6, 35050−35056

to adjust the focus at the central depth of the droplet to show the outskirts of the droplet under brightfield illumination.

Raman microscopy (Lamda Vision) was used for the characterization of chemicals inside the droplets. The excitation laser has a wavelength of 532 nm (MLL-III-532) with an intensity of 30 mW. The magnification of the objective lens was 40×, and a typical resolution of this microscope was ∼5 μm.

The pendant drop method (DMs-401, Kyowa Kaimen Kagaku) was utilized to monitor the interfacial tension for an LC droplet in a solution. The sample was prepared via a pendant drop (15 μL) of 5CB from a syringe needle into a measurement cell filled with an SDS solution with solute molecules. The image sequence of the pendant drop was acquired by a camera every second, and each interfacial tension was calculated from the droplet shape by fitting with the Young−Laplace equation.

DATA AVAILABILITY

The data that support the findings of this study are available from the corresponding author upon reasonable request.

ASSOCIATED CONTENT

Supporting Information

The Supporting Information is available free of charge at https://pubs.acs.org/doi/10.1021/acsomega.1c05816.

Photocrystallization of *p*-nitrophenol in 5CB; photocrystallization of *p*-nitrophenol in 5CB under crossed-Nicols condition; photocrystallization of alizarin yellow in 5CB; photocrystallization of chrome yellow in 5CB; 5CB droplet in a PVA solution under UV irradiation; 5CB droplet in an SDS solution in an isotropic state under UV irradiation; toluene droplet in an SDS solution under UV irradiation; 5CB droplet in an SDS solution during heating (mp4) (ZIP)

UV/Vis change of *p*-nitrophenol with a 5CB droplet and under UV irradiation; contact angle dependence of a 5CB droplet on the *p*-nitrophenol concentration; microfluidic device for formation of 5CB droplets; UV/Vis absorption spectra of solute molecules; microscopy setup of the droplets; schematic of the microfluidic device consisting of a glass capillary, geometry of microcapillaries, and formation mechanism of a single emulsion; UV/Vis absorption spectra of p-nitrophenol, alizarin yellow GG, and chrome yellow; and schematic drawing of the observation setup (PDF)

AUTHOR INFORMATION

Corresponding Author

Kenji Katayama − *Department of Applied Chemistry, Chuo University, Tokyo 112-8551, Japan;* orcid.org/0000-0003-3278-6485; Phone: +81-3-3817-1913; Email: kkata@kc.chuo-u.ac.jp

Authors

Yota Sakai − *Department of Applied Chemistry, Chuo University, Tokyo 112-8551, Japan*

Hinako Kusaki − *Department of Applied Chemistry, Chuo University, Tokyo 112-8551, Japan*

Complete contact information is available at: https://pubs.acs.org/10.1021/acsomega.1c05816

Author Contributions

Y.S. and K.K. designed the experiments and analyzed results and wrote the paper. H.K. prepared samples and made observations.

Notes

The authors declare no competing financial interest.

ACKNOWLEDGMENTS

This research was supported by the Institute of Science and Engineering, Chuo University. We appreciate R. Sakai for supporting the microscopic observation.

REFERENCES

(1) LaMer, V. K.; Dinegar, R. H. Theory, Production and Mechanism of Formation of Monodispersed Hydrosols. *J. Am. Chem. Soc.* **1950**, *72*, 4847−4854.

(2) Gao, Z.; Rohani, S.; Gong, J.; Wang, J. Recent Developments in the Crystallization Process: Toward the Pharmaceutical Industry. *Engineering* **2017**, *3*, 343−353.

(3) Yang, Y.; Nagy, Z. K. Advanced Control Approaches for Combined Cooling/Antisolvent Crystallization in Continuous Mixed Suspension Mixed Product Removal Cascade Crystallizers. *Chem. Eng. Sci.* **2015**, *127*, 362−373.

(4) Alvarez, A. J.; Myerson, A. S. Continuous Plug Flow Crystallization of Pharmaceutical Compounds. *Cryst. Growth Des.* **2010**, *10*, 2219−2228.

(5) McGlone, T.; Briggs, N. E. B.; Clark, C. A.; Brown, C. J.; Sefcik, J.; Florence, A. J. Oscillatory Flow Reactors (OFRs) for Continuous Manufacturing and Crystallization. *Org. Process Res. Dev.* **2015**, *19*, 1186−1202.

(6) Hoshino, M.; Khutia, A.; Xing, H.; Inokuma, Y.; Fujita, M. The Crystalline Sponge Method Updated. *IUCrJ* **2016**, *3*, 139−151.

(7) Inokuma, Y.; Yoshioka, S.; Ariyoshi, J.; Arai, T.; Hitora, Y.; Takada, K.; Matsunaga, S.; Rissanen, K.; Fujita, M. X-Ray Analysis on the Nanogram to Microgram Scale Using Porous Complexes. *Nature* **2013**, *495*, 461−466.

(8) Yuyama, K.-i.; Rungsimanon, T.; Sugiyama, T.; Masuhara, H. Selective Fabrication of α- and γ-Polymorphs of Glycine by Intense Polarized Continuous Wave Laser Beams. *Cryst. Growth Des.* **2012**, *12*, 2427−2434.

(9) Hua, T.; Valentín-Valentín, C.; Gowayed, O.; Lee, S.; Garetz, B. A.; Hartman, R. L. Microfluidic Laser-Induced Nucleation of Supersaturated Aqueous Glycine Solutions. *Cryst. Growth Des.* **2020**, *20*, 6502−6509.

(10) Mitov, M. Cholesteric Liquid Crystals in Living Matter. *Soft Matter* **2017**, *13*, 4176−4209.

(11) Nersisyan, S. R.; Tabiryan, N. V. Polarization Imaging Components Based on Patterned Photoalignment. *Mol. Cryst. Liq. Cryst.* **2008**, *489*, 156−168.

(12) Nersisyan, S.; Tabiryan, N.; Steeves, D. M.; Kimball, B. R. Fabrication of Liquid Crystal Polymer Axial Waveplates for UV-IR Wavelengths. *Opt. Express* **2009**, *17*, 11926−11934.

(13) Wu, H.; Hu, W.; Hu, H.-c.; Lin, X.-w.; Zhu, G.; Choi, J.-W.; Chigrinov, V.; Lu, Y.-q. Arbitrary Photo-Patterning in Liquid Crystal Alignments Using DMD Based Lithography System. *Opt. Express* **2012**, *20*, 16684−16689.

(14) Lopez-Leon, T.; Fernandez-Nieves, A. Drops and Shells of Liquid Crystal. *Colloid Polym. Sci.* **2011**, *289*, 345−359.

(15) Wang, X.; Miller, D. S.; Bukusoglu, E.; de Pablo, J. J.; Abbott, N. L. Topological Defects in Liquid Crystals as Templates for Molecular Self-Assembly. *Nat. Mater.* **2016**, *15*, 106−112.

(16) Kawaguchi, K.; Kageyama, R.; Sano, M. Topological Defects Control Collective Dynamics in Neural Progenitor Cell Cultures. *Nature* **2017**, *545*, 327−331.

(17) Saw, T. B.; Doostmohammadi, A.; Nier, V.; Kocgozlu, L.; Thampi, S.; Toyama, Y.; Marcq, P.; Lim, C. T.; Yeomans, J. M.;

Ladoux, B. Topological Defects in Epithelia Govern Cell Death and Extrusion. *Nature* **2017**, *544*, 212−216.
(18) Liu, Q.; Cui, Y.; Gardner, D.; Li, X.; He, S.; Smalyukh, I. I. Self-Alignment of Plasmonic Gold Nanorods in Reconfigurable Anisotropic Fluids for Tunable Bulk Metamaterial Applications. *Nano Lett.* **2010**, *10*, 1347−1353.
(19) Milette, J.; Relaix, S.; Lavigne, C.; Toader, V.; Cowling, S. J.; Saez, I. M.; Lennox, R. B.; Goodby, J. W.; Reven, L. Reversible Long-Range Patterning of Gold Nanoparticles by Smectic Liquid Crystals. *Soft Matter* **2012**, *8*, 6593−6598.
(20) Coursault, D.; Grand, J.; Zappone, B.; Ayeb, H.; Lévi, G.; Félidj, N.; Lacaze, E. Linear Self-Assembly of Nanoparticles Within Liquid Crystal Defect Arrays. *Adv. Mater.* **2012**, *24*, 1461−1465.
(21) Pires, D.; Fleury, J.-B.; Galerne, Y. Colloid Particles in the Interaction Field of a Disclination Line in a Nematic Phase. *Phys. Rev. Lett.* **2007**, *98*, 247801.
(22) Wood, T. A.; Lintuvuori, J. S.; Schofield, A. B.; Marenduzzo, D.; Poon, W. C. K. A Self-Quenched Defect Glass in a Colloid-Nematic Liquid Crystal Composite. *Science* **2011**, *334*, 79−83.
(23) Tkalec, U.; Ravnik, M.; Čopar, S.; Žumer, S.; Muševič, I. Reconfigurable Knots and Links in Chiral Nematic Colloids. *Science* **2011**, *333*, 62−65.
(24) Sakai, Y.; Sohn, W. Y.; Katayama, K. Optical Motion Control of Liquid Crystalline Droplets by Host−Guest Molecular Interaction. *Soft Matter* **2019**, *15*, 7159−7165.
(25) Dogishi, Y.; Sakai, Y.; Sohn, W. Y.; Katayama, K. Optically Induced Motion of Liquid Crystalline Droplets. *Soft Matter* **2018**, *14*, 8085−8089.
(26) Sakai, Y.; Sohn, W. Y.; Katayama, K. Photo-Controllable Rotational Motion of Cholesteric Liquid Crystalline Droplets in a Dispersion System. *RSC Adv.* **2020**, *10*, 21191−21197.
(27) Syme, C. D.; Mosses, J.; González-Jiménez, M.; Shebanova, O.; Walton, F.; Wynne, K. Frustration of Crystallisation by a Liquid−Crystal Phase. *Sci. Rep.* **2017**, *7*, 42439.
(28) Wang, D.; Park, S.-Y.; Kang, I.-K. Liquid Crystals: Emerging Materials for Use in Real-Time Detection Applications. *J. Mater. Chem. C* **2015**, *3*, 9038−9047.
(29) Prishchepa, O. O.; Shabanov, A. V.; Zyryanov, V. Y. Director Configurations in Nematic Droplets with Inhomogeneous Boundary Conditions. *Phys. Rev. E: Stat., Nonlinear, Soft Matter Phys.* **2005**, *72*, 031712.
(30) Bushuyev, O. S.; Friščić, T.; Barrett, C. J. Controlling Dichroism of Molecular Crystals by Cocrystallization. *Cryst. Growth Des.* **2016**, *16*, 541−545.

https://doi.org/10.1021/acsomega.1c05816
ACS Omega 2021, 6, 35050−35056